ASSESSMENT OF TURBULENT MODELLING FOR CFD SIMULATION IN HYDROTURBINES: DRAFT TUBES

Marcelo Dias de Moura
mdmoura@unb.br
Antônio C. P. Brasil Júnior
brasiljr@unb.br
Universidade de Brasília - Campus Darcy Ribeiro - Faculdade de Tecnologia
Departamento de Engenharia Mecânica - Laboratório de Energia e Ambiente - Brasília-DF, CEP 70.910-900

Abstract. *The study of the draft tube flow has great importance to predict the behaviour in hydroturbines, whereas the effectiveness and the power are significantly affected by performance of its draft tube. The aim of this work is modelling, simulation and characterization of tridimensional flow in the draft tube of hydroturbines. The flow investigation is made through simulations of several turbulence models using a commercial software CFX 5.6, based on the finite volume method with a hexahedral mesh generated in the mesh generator ICEM CFD 4.2.2. Qualitatives and quantitatives results validation are proved by workshops benchmark experiments, in order these results can obtain a turbulence model that represents the flow complexity in draft tubes.*

Keywords: *Numerical simulation, draft tube, CFD, Turbulence Models.*

1. Introduction

The aim of this study is based on modelling, simulation and characterization of the complex, unstable and three-dimensional flow of the draft tube, from of the analysis of the fluid behavior from the runner outlet until the draft tube outlet and an evaluation of the capacity of the numeric simulations on CFD programs, CFX 5.6 (AEA Technology).

A set of experimental information was found in the workshop *Turbine 99* I and II, accomplished in Sweden in 1999 and 2001 for the draft tube of a turbine Kaplan. The database generated by the two workshops was organized to determine the state-of-the-art of the simulation in CFD of the draft tube flow (Bergström (1999)). A base of information of the experimental study on the draft tube can be found in Andersson & Karlsson (1999). Models of high order were tested for the draft tube in Grotjans (1999). Avellan *et al.* (2002), tried to test the influence of the boundary conditions in the draft tube, evaluating the capacity of the numeric simulation to predict the flow, showing a detailed comparison of the measurements with experimental data, in order to verify and validate the approach the turbulence models.

The results found in comparison with quantitative data (non-dimensional parameters that define the draft tube efficiency) and qualitative (flow topology) showed that the simpler models ($KE1E$, $k-\varepsilon$ and $k-\omega$) showed more agreement in the draft tube flow of the workshop *Turbine 99*.

1.1 Boundary Conditions

The motivation for the choice of the draft tube was, mainly, because most of the hydroelectric power stations in Sweden were modeled for low head, so most of the energy losses are related to the draft tube (Bergström (2000)). The chosen plant was the hydroelectric of Hölleforsen, located in the river Indals built in 1941. The real turbine has a head of $24.9\ m$, rotating with $125\ rpm$, a volume flow of $149\ m^3/s$. The turbine model, in $1:11$ scale, has a head of $4.5\ m$, runner speed of $595\ rpm$, volume flow of $0.533\ m^3/s$.

As the velocity as the axissimetrical Reynolds stress components were considered in the inlet, what implies that those values become dependent of the position along the angle θ in the inlet of the draft tube. Besides, the flow is rotating in the draft tube inlet, due to the imposition of the runner turn, leaving with a constant pressure and close to the atmospheric pressure value. The velocity components had to be converted in function of the angle θ instead the cartesian coordinates in the inlet of the draft tube:

$$\begin{cases} u = Result(\cos\theta) \\ v = -Result(\sin\theta) \\ w = w_{axial} \end{cases} \tag{1}$$

where $Result$, the resultant between the radial vectors and tangential; u, v and w the velocity components in the x, y and z direction, respectively.

The radial velocity at the inlet is unknown. It was calculated in function of the axial velocity measurement, considering that the velocity vector is related to be parallel to the wall runner cone and the draft tube wall. Consequently the following radial velocity will be used at the inlet:

$$U_{radial} = U_{axial}\tan\theta_o \tag{2}$$

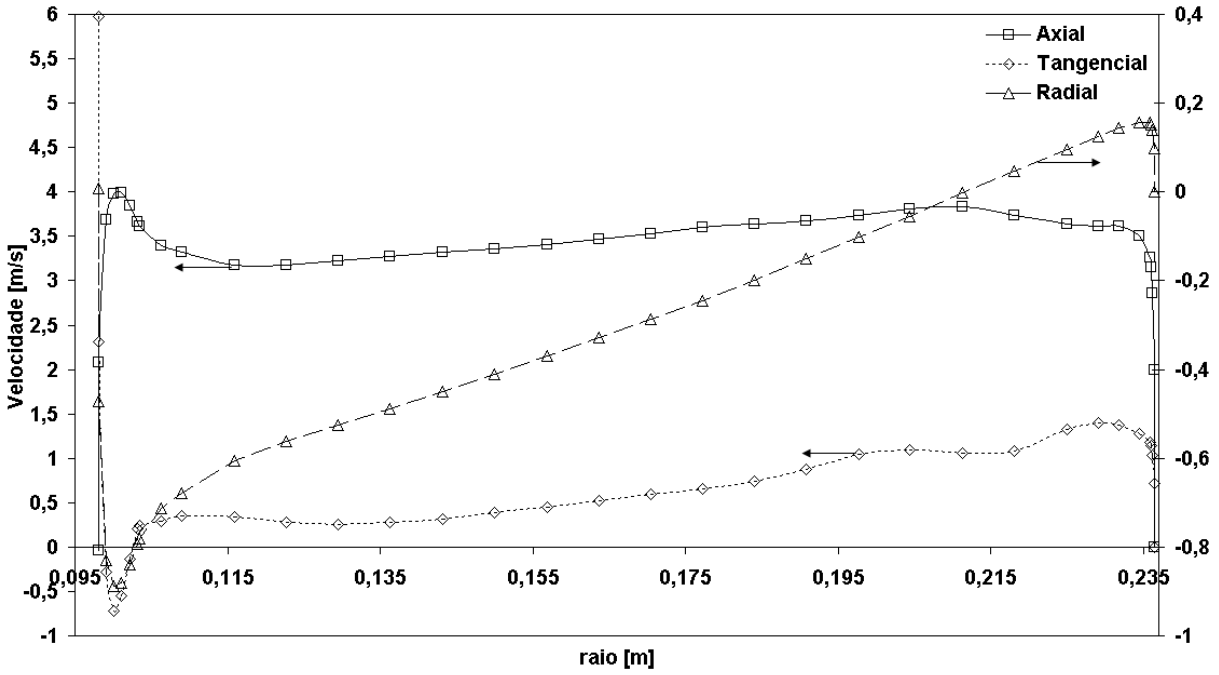

Figure 1. Experimental Measurements (LDV) in Operation Mode T (Best efficiency): Velocity Components;

where

$$\theta_o = \theta_{cone} + \frac{\theta_{wall} - \theta_{cone}}{R_{wall} - R_{cone}}(r - R_{cone}) \tag{3}$$

and $r = \sqrt{x^2 + y^2}$, $R_{cone} \leq r \leq R_{wall}$, $\theta_{cone} = -12.8°$ and $\theta_{wall} = 2.8°$. θ_o is the angle of the flow in the vertical plane and is equal to zero for the plane z. Where U_{axial} is the axial velocity of the measurements.

The wall condition at the tube was adopted as being with no-slipping condition and roughness of $0.1\ \mu m$. For the wall at the runner cone it was also used no slipping condition. But, as the cone rotates with the runner, the velocity applied as tangential was used on the cone wall. At the draft tube outlet, it was made an approach considering the static pressure at the outlet as constant and equal to zero.

1.2 Mathematical Formulation

The flow of an incompressible and turbulent fluid is described by mass conservation and momentum equations and can be expressed by the Reynolds average equations, as following:

$$\nabla \cdot \mathbf{U} = 0 \tag{4}$$

$$\frac{\partial \mathbf{U}}{\partial t} + (\nabla \mathbf{U})\mathbf{U} = -\frac{1}{\rho}\nabla P + \nabla \cdot (\nu \nabla \mathbf{U}) - \nabla \cdot (\overline{\mathbf{u}' \otimes \mathbf{u}'}) \tag{5}$$

where $\mathbf{U}$ and P are the average velocity and the pressure field; ρ and ν are the density and the kinematic viscosity of the fluid respectively; and $\overline{\mathbf{u}' \otimes \mathbf{u}'}$ is the Reynolds stress modeled by the hypothesis of Boussinesq eddy viscosity:

$$-\overline{\mathbf{u}' \otimes \mathbf{u}'} = 2\nu_t \mathbf{S(u)} - \frac{2}{3}(k\mathbf{I}) \tag{6}$$

where ν_t is the eddy viscosity, **S(u)** is the symmetrical part of the velocity gradient stress, **I** is it identity tensor and k is the turbulent kinetic energy.

Along the last decades a great diversity of turbulence models has been proposed, it is due to the progress of the computacional field providing the creation and simulation of more complex models.

1.3 One Equation Model

A formalism is presented in the work of Menter (1994) that allows a transformation of the models of turbulent viscosity from two equations of turbulence models into one equation. In order to achieve the models of one equation, Menter

followed the work of Baldwin & Barth (1990) and expressed the time derivative of the eddy viscosity by the time derivatives of k and ε of the model $k-\varepsilon$ standard. Substituting the total derivative of k and ε , we can achieve into one simple transport equation for the eddy viscosity, that, however, depends on k and ε as well as the eddy viscosity.

The final form of the equation is:

$$\frac{D\tilde{\nu}_t}{Dt} = c_1 D_1 \tilde{\nu}_t \Omega - c_2 E_{1e} + \frac{\partial}{\partial x_j}\left[\left(\nu + \frac{\tilde{\nu}_t}{\sigma}\right)\frac{\partial}{\partial x_j}(\tilde{\nu}_t)\right] \tag{7}$$

$$\hat{c}_1 = (c_{\varepsilon 2} - c_{\varepsilon 1})\sqrt{c_\mu} = 0,24 \qquad \hat{\sigma} = \sigma_\varepsilon = 0,7 \qquad \hat{c}_2 = \frac{\hat{c}_1}{\kappa^2} + \frac{1}{\hat{\sigma}} = 2,86 \tag{8}$$

They are based on $c_{\varepsilon 1} = 1,2$, $c_{\varepsilon 2} = 2,0$, $c_\mu = 0,09 = a_1^2$ e $\sigma_\varepsilon = 0,7$ for the model $k-\varepsilon$ standard.

1.4 Two Equation Models

The $k-\varepsilon$ model assumes that the eddy viscosity related with the turbulent kinetic energy and the dissipation through the relationship:

$$\mu_t = c_\mu \rho \frac{k^2}{\varepsilon} \tag{9}$$

where c_μ is a constant and equal to 0.09. The values of k and ε come directly from the transport equations of the turbulent kinetic energy and from turbulence dissipation rate:

$$\frac{\partial \rho k}{\partial t} + \nabla \cdot (\rho \mathbf{U} k) - \nabla \cdot \left(\frac{\mu_{ef}}{\sigma_k}\nabla k\right) = P_k - \rho\varepsilon \tag{10}$$

$$\frac{\partial \rho \varepsilon}{\partial t} + \nabla \cdot (\rho \mathbf{U} \varepsilon) - \nabla \cdot \left(\frac{\mu_{ef}}{\sigma_\varepsilon}\nabla \varepsilon\right) = \frac{\varepsilon}{k}(c_{\varepsilon 1} P_k - c_{\varepsilon 2}\rho\varepsilon) \tag{11}$$

where $c_{\varepsilon 1} = 1,44$, $c_{\varepsilon 2} = 1,92$, $\sigma_k = 1$ and $\sigma_k = 1,3$ are constants of the problem.

The initial point of the present formulation of the $k-\omega$ model was developed by Wilcox (1986). Solving two transport equations, one for the turbulent kinetic energy, k, and one for the turbulent frequency, ω. The shear stress is calculated by the specific viscosity concept μ_t, ρ, and the velocity, $\mathbf{U}$, are treated as known quantities from the Navier-Stokes method.

The format of the equations is a lot similar to the model $k-\varepsilon$ and the turbulent viscosity hypothesis of $k-\omega$ model it consists of:

1. Turbulent Viscosity Specification:

$$\nu_t = \frac{k}{\omega} \tag{12}$$

2. Turbulent Kinetic Energy Transport Equation, k:

$$\frac{\partial k}{\partial t} + \mathbf{U}\cdot\nabla k = \nabla \cdot [(\nu + \nu_t \sigma^*)\nabla k] + \tau : \nabla \mathbf{U} - \beta^* k\omega \tag{13}$$

3. Specific Dissipation Rate for Transport Equation, ω:

$$\frac{\partial \omega}{\partial t} + \mathbf{U}\cdot\nabla \omega = \nabla \cdot [(\nu + \nu_t \sigma)\nabla \omega] + \alpha\frac{\omega}{k}\tau : \nabla \mathbf{U} - \beta\omega^2 \tag{14}$$

where the coefficients closure are:

$$\alpha = \frac{5}{9}, \quad \beta = \frac{3}{40}, \quad \beta^* = \frac{9}{100}, \quad \sigma = \frac{1}{2} \quad \text{e} \quad \sigma^* = \frac{1}{2} \tag{15}$$

An improvement in terms of predict of separation of the flow has been gotten by the model $k-\omega$ based on SST (Shear Stress Transport). The own transport behavior can be obtained by a limitator for the eddy viscosity formulation:

$$\nu_t = \frac{a_1 k}{\max(a_1\omega, SF_2)} \tag{16}$$

Again F_2 is a blending function similar to F_1, which restricts the limiter to the wall boundary layer, as the underlying assumptions are not correct for free shear flows. S is an invariant measure of the strain rate.

The blending functions are critical to the success of the method. Their formulation is based on the distance to the nearest surface and on the flow variables:

$$F_1 = \tanh(\arg_1^4) \quad \arg_1 = \min\left[\max\left(\frac{\sqrt{k}}{\beta'\omega}, \frac{500\nu}{y^2\omega}\right), \frac{4\rho\sigma_{\omega 2}k}{CD_{k\omega}y^2}\right] \tag{17}$$

where:

$$CD_{k\omega} = \max(2\rho\sigma_{\omega 2}\frac{1}{\omega}\nabla k\nabla\omega, 1, 0.10^{-10}) \quad F_2 = \tanh(\arg_2^2) \quad arg_2 = \max\left(\frac{2\sqrt{k}}{\beta'\omega y}, \frac{500\nu}{y^2\omega}\right) \tag{18}$$

1.5 Results and Discussions

Numeric simulations are intended to be done to approach the experimental data as close as possible. One of the points that defines the accuracy of the results is the mesh to be chosen. Three types of mesh discretization of mesh were elaborated, using the multi-block process, which can be obtained by local refinement. With base in the comparison of pressure data and velocity, the chosen mesh was the one of 735352 elements (Fig. (2)) with level of convergence of 10^{-5}.

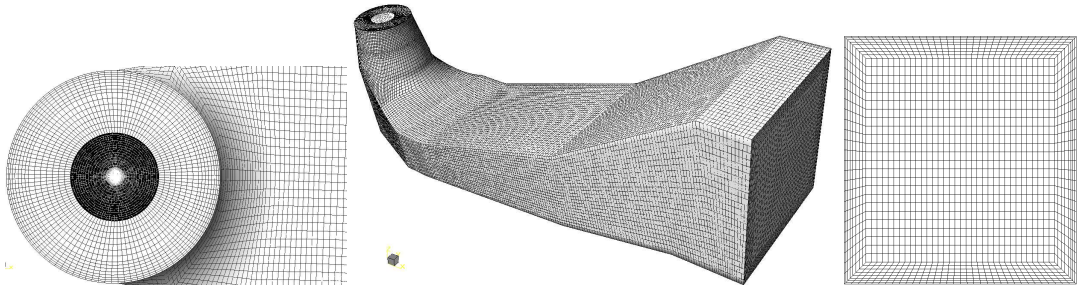

Figure 2. Visualization of the Mesh of 735352 Hexahedral Elements.

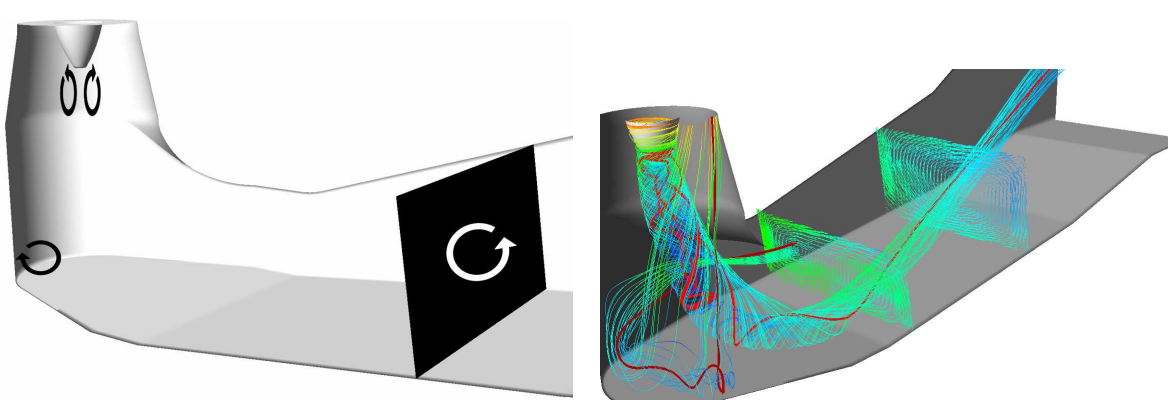

Figure 3. Secondary flow based on Information of the Experiments and Visualization of the Vortexes Generated by the Runner and for the Geometry of the Draft Tube.

Tab. (1) shows the CPU time for each model to reach the convergence level adopted.

As it seen as previously, the draft tube has the objective to gain part of the pressure energy, lost during the operation of the machine, avoiding as possible losses that may happen at the tube inlet and at the outlet. The efficiency operation of the tube can be translated through several non-dimensional factors. The first of them is the pressure coefficient visualized through the center lines located at the bottom and top of the tube. The comparison with the pressure coefficient measurements at the top and bottom center lines (Fig. (4) and Fig. (5)) showed good agreement except for one pressure jump in a part of the bottom line as well as the top one. The pressure jump in the top center line happens in the end of the first conical section of the draft tube. The reason of the discrepancy in this area is probably because the mesh isn't enough refined to solve this jump. The area of high pressure in the bottom line consists of two peaks, the first to the left and a more dispersed second. Visualizations done by Andersson & Karlsson (1999) showed that there is a big vortex in this edge. The models with better results were the simplest models, based on the eddy viscosity showed in Fig. (4a) and Fig. (5a), except for the model the zero equation that over predict the value of C_p to the long of the tube. A special highlight to the model $k-\varepsilon$, which obtained the best results at the top center line as well as the bottom center line of the tube.

Other parameters regarding the tube are also compared for each model, as shown in Tab. (2). In the study of the draft tube the calculation of several parameters is necessary to obtain a quantitative result of its efficiency, in which refers

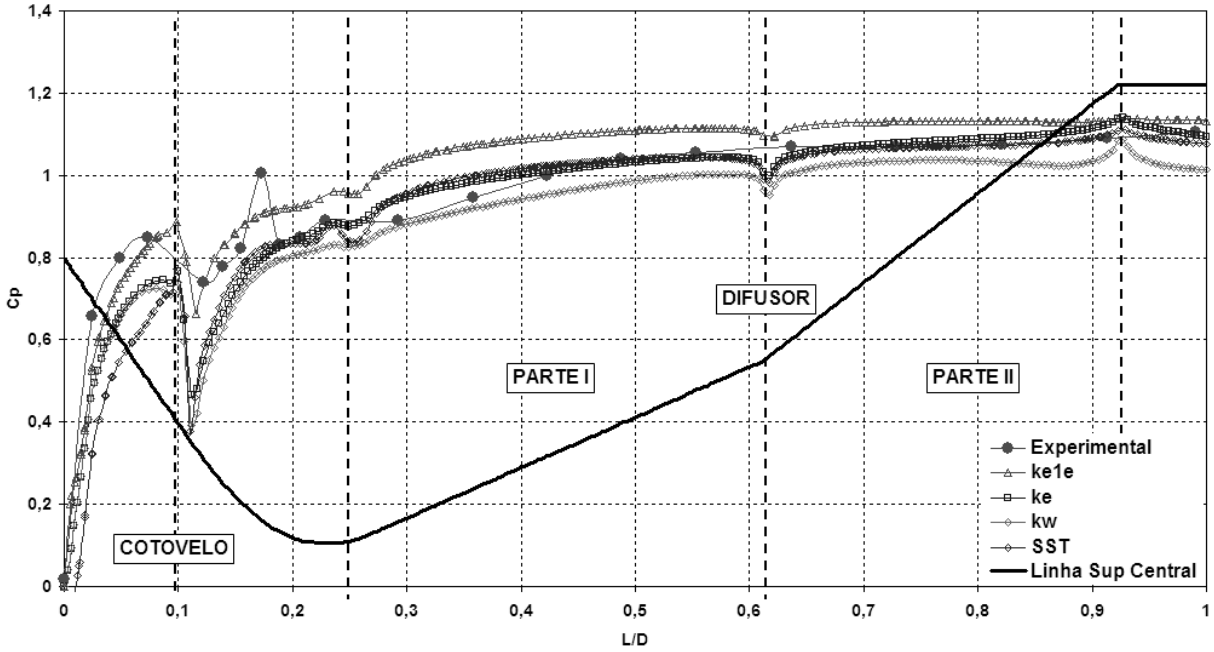

Figure 4. Pressure Coefficient Comparison at the top centerline.

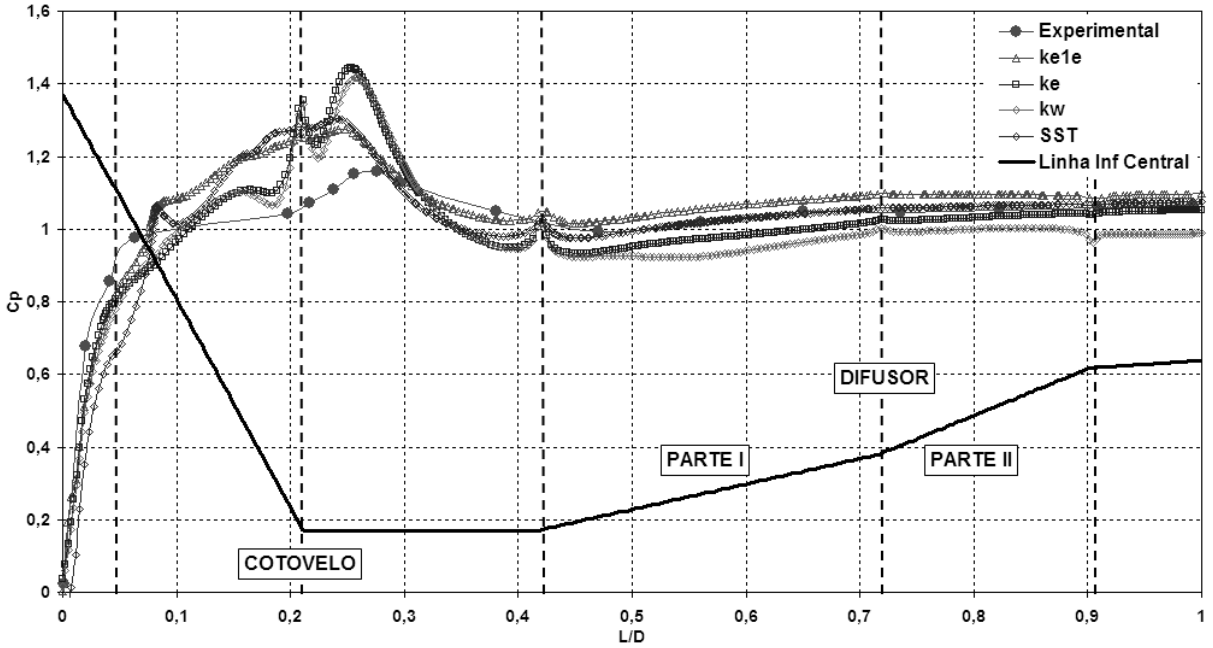

Figure 5. Pressure Coefficient Comparison at the bottom centerline.

to recover the kinetic energy and the degree of non-uniformity of the flow. The pressure recovery factor indicates the conversion degree of the kinetic energy in static pressure where high value means a high efficiency for the draft tube. The coefficient ζ is directly connected to the losses in the system, where a small value means high efficiency for the draft tube. For the coefficient of pressure recovery (C_{pr}) the models that presented better results were $KE1E$, the $k-\varepsilon$ and the model $k-\omega$. The correction of energy swirl kinetics factor just the models $k-\omega$ and the model SST presented good agreement. In relation to the correction factor of momentum, again the models $k-\varepsilon$ and the model SST were closer to the experimental results.

Firstly we will compare the tangential velocities, according to experimental information, as showed at the Andersson & Karlsson (1999) work, there is just the presence of a great vortex rotating in the counterclockwise direction. The models that presented better agreement with the experimental information are the $KE1E$ and $k-\varepsilon$ models, with the difference that in the model $k-\varepsilon$ the vortex is located more in the center of the section while the $KE1E$ model the vortex is more

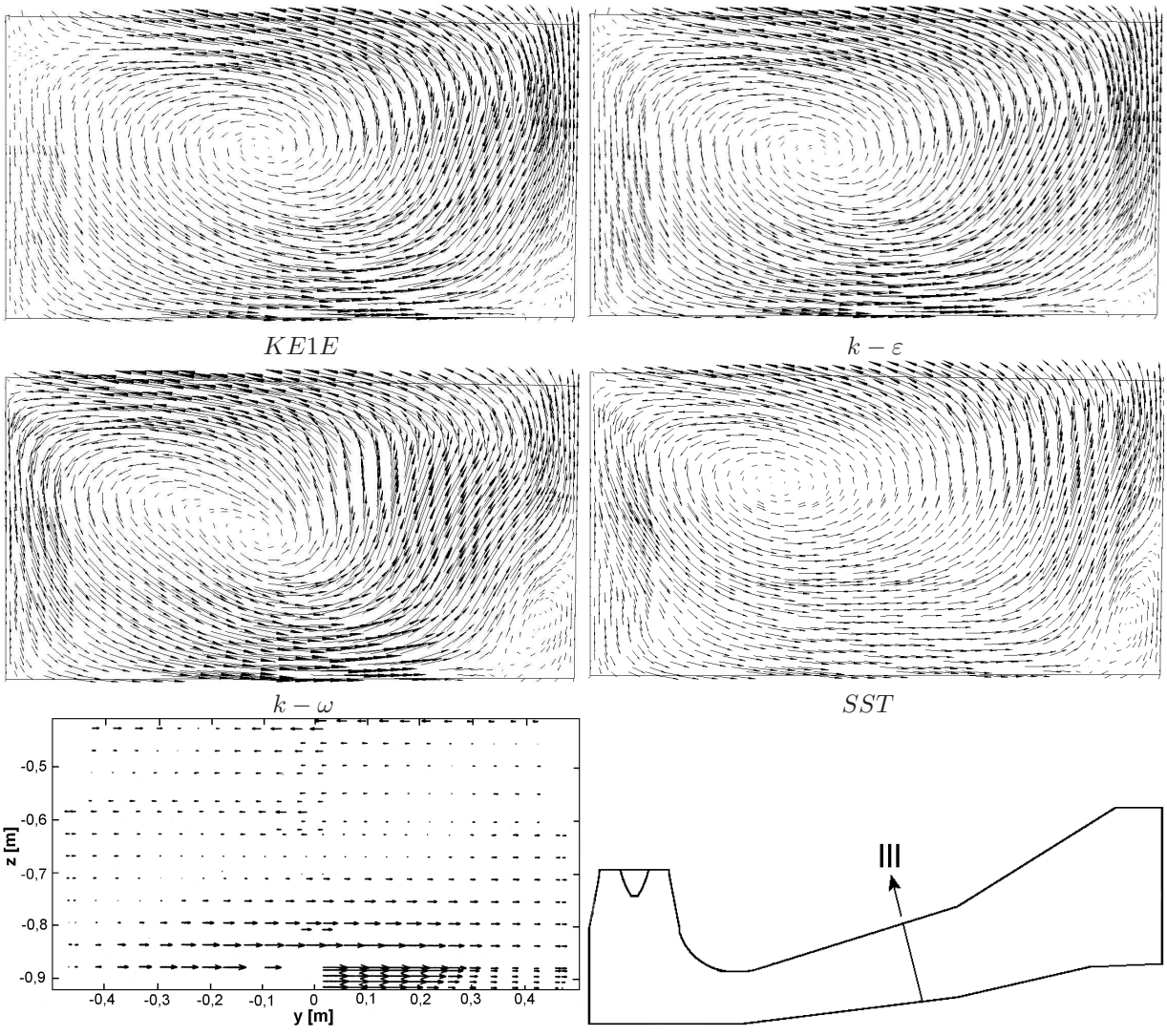

Experimental Measurement Section

Figure 6. Tangential Vectors in the Plane III

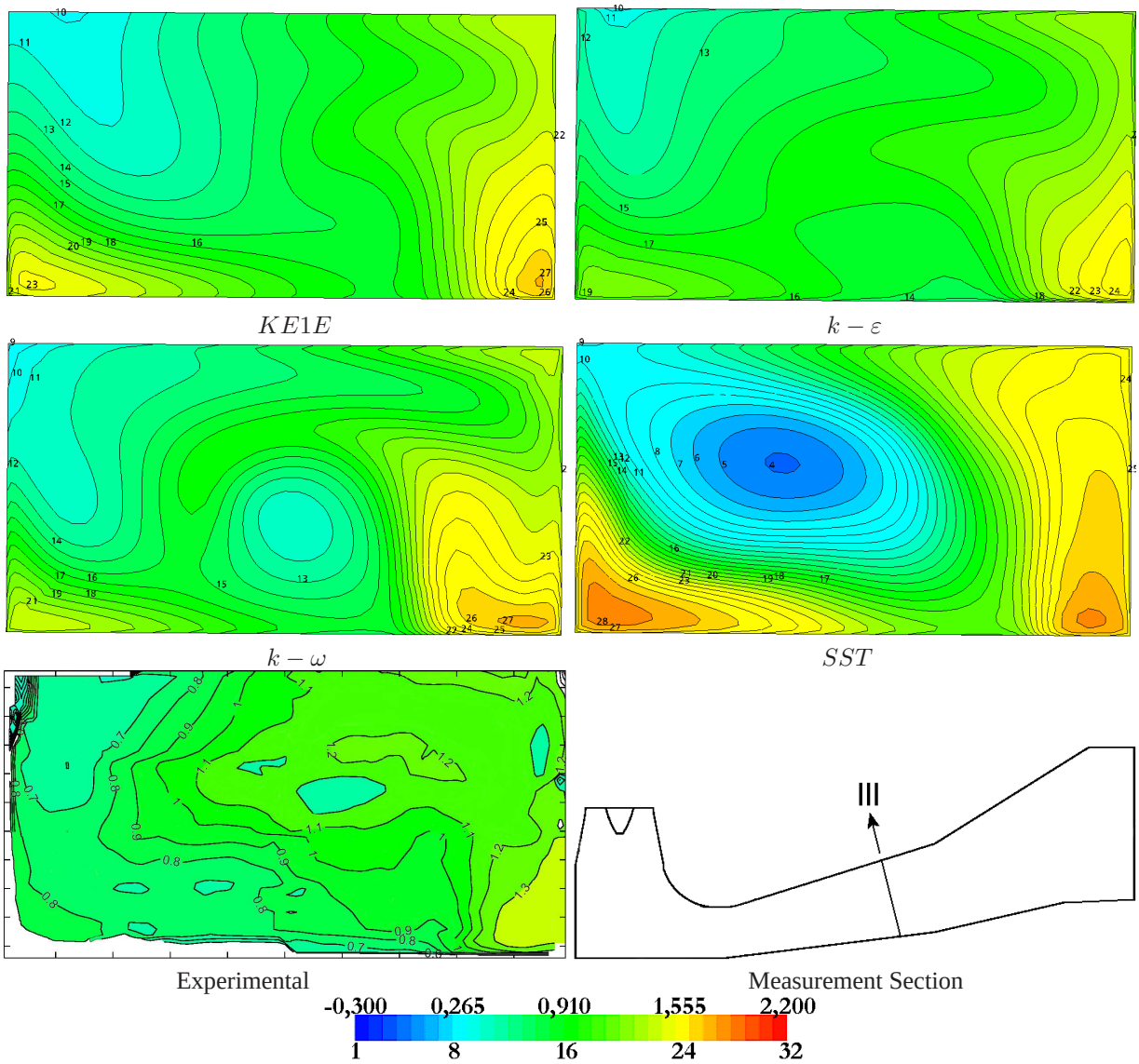

Figure 7. Isolines of the Velocity Component u in the Plane III.

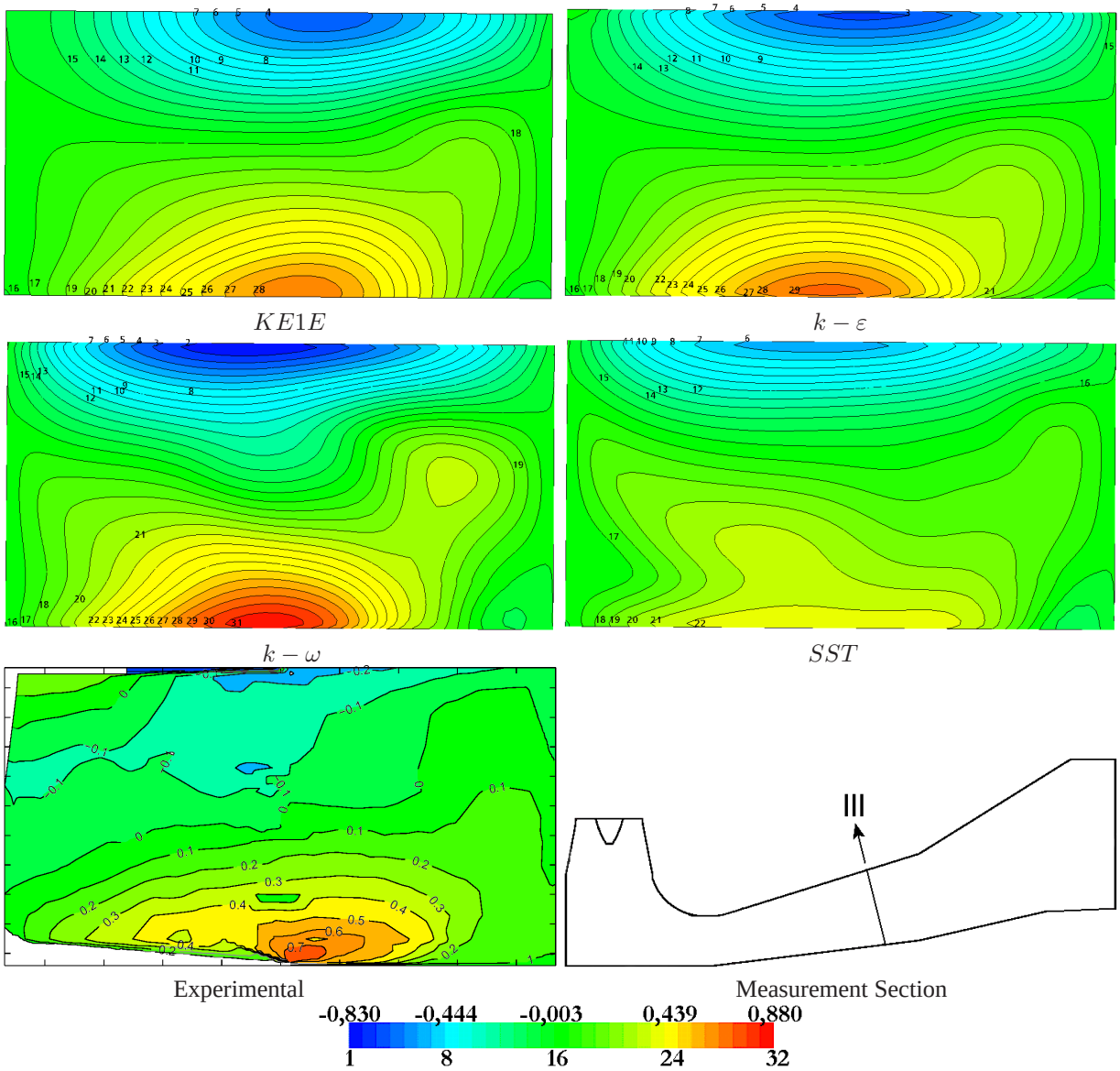

Figure 8. Isolines of the Velocity Component v in the Plane III.

Table 1. Time of CPU and Level of Convergence of the Tested Models.

Model	$N^{\underline{o}}$ of Iterations	Time of CPU	Convergence
$kE1E$	130	6 h 25 min	
$k-\varepsilon$	104	5 h 14 min	
$k-\omega$	88	4 h 25 min	
SST	102	5 h 35 min	10^{-5}

Table 2. Comparison of the Parameters of the Draft Tube for the Turbulence Models.

Formula	$k-\varepsilon$	$k-\omega$	SST	$KE1E$	Exper.
$C_{pr}=\frac{P_{Parede-Saída}-P_{Parede-Entrada}}{\frac{1}{2}\rho U^2_{axial-Entrada}}$	1,07	1,0	0,802	1,115	1,12
$\zeta=\frac{\iint_{A_{Entrada}}\left(P+\rho\frac{\lvert\mathbf{u}\rvert^2}{2}\right)\mathbf{u}\cdot\hat{\mathbf{n}}dA+\iint_{A_{Saída}}\left(P+\rho\frac{\lvert\mathbf{u}\rvert^2}{2}\right)\mathbf{u}\cdot\hat{\mathbf{n}}dA}{\left\lvert\iint_{A_{Entrada}}\rho\frac{\lvert\mathbf{u}\rvert^2}{2}\mathbf{u}\cdot\hat{\mathbf{n}}dA\right\rvert}$	0,33753	0,39193	0,49849	0,40602	-
$\alpha_{axial-Ia}=\frac{1}{A\overline{u}^3_{axial}}\int_A u^3_{axial}\,dA$	1,05319	1,05297	1,05291	1,05353	1,03
$\alpha_{axial-III}=\frac{1}{A\overline{u}^3_{axial}}\int_A u^3_{axial}\,dA$	1,11599	1,21828	1,01507	0,90747	1,09
$\alpha_{swirl-Ia}=\frac{1}{A\overline{u}^3_{axial}}\int_A u^2_{tang}u_{axial}\,dA$	0,03883	0,03882	0,03880	0,03888	0,06
$\alpha_{swirl-III}=\frac{1}{A\overline{u}^3_{axial}}\int_A u^2_{tang}u_{axial}\,dA$	0,02474	0,04138	0,04111	0,02907	0,04
$\beta_{Ia}=\frac{1}{A\overline{u}^2_{axial}}\int_A u^2\,dA$	1,11155	1,11134	1,11133	1,11183	1,02
$\beta_{III}=\frac{1}{A\overline{u}^2_{axial}}\int_A u^2\,dA$	1,07590	1,14068	1,01001	0,93728	1,02
$S_{Ia}=\frac{1}{R}\frac{\int_A[u_{tang}r(\rho u_{axial})]\,dA}{\rho\int_A u_{axial}\,dA}$	0,29950	0,29950	0,29950	0,29950	0,31
$S_{III}=\frac{1}{R}\frac{\int_A[u_{tang}r(\rho u_{axial})]\,dA}{\rho\int_A u_{axial}\,dA}$	0,51442	0,48776	0,34875	0,42223	-

to the left of the plane (Fig. 6). The $k-\omega$ and SST models show a second vortex in the bottom of the left edge. The velocity component v (Fig. 8) has better agreement with almost all models. Already for the component u (Fig. 7), just the $KE1E$, $k-\varepsilon$ and $k-\omega$ models presented good agreement. The $KE1E$, $k-\varepsilon$ and $k-\omega$ models were the models that showed better agreement as well as the flow topology, as in the magnitude of the velocity along the section. The SST model presented good agreement as the flow topology for this velocity component, but in relation to the maximum velocity in the bottom of the tube, it was relatively lower than experimental information.

2. Conclusions

The present work tried to validate turbulence models available in the CFD codes that were applied to the draft tube of the Kaplan turbine in showed at the workshop *Turbine 99*, and verify that are the which models predicts a better flow quality. Non-dimensional parameters (C_{pr}, ζ, α_{axial}, α_{swirl}, S, etc.), draft tube characteristic and velocity components were compared with the workshop results. The simplest models, $KE1E$, $k-\varepsilon$, $k-\omega$ and SST presented good agreement relating to several correction factors to measure the efficiency of the draft tube. It is missing of information on the Reynolds stress components for the boundary conditions of the draft tube did with the Reynolds stress models didn't obtain good results.

3. References

AEA Technology, 2001, "CFX 5: Introductory Tutorials" Didcot Oxfordshire OX11 OQR, Unit Kingdom.

Andersson, U. and Karlsson, R., 1999, "Quality Aspects of the Turbine 99 Draft Tube Experiment" in Proceedings of Turbine-99 - Workshop on draft tube flow in Porjus, Sweden, 20-23 June 1999.

Avellan, F., Kueny, J. L. and Murie, S., 2002, "Werlé-Legendre Separation in a Hydraulic Machine Draft Tube", in Proceedings of ASME FEDSM'02, Quebec, Canada, 14-18 de Julho, 2002.

Bergström, J., 1999, "Approximations of Numerical Errors and Boundary Conditions in a Draft Tube", Proceeding of Turbine-99 - Workshop on Draft Tube Flow in Porjus, Sweden, 20-23 June 1999.

Grotjans, H., 1999, "Higher Order Turbulence Modelling for Draft Tube Applications", in Proceeding of Turbine-99 - Workshop on Draft Tube Flow in Porjus, Sweden, 20-23 June 1999.

Maliska, C. R., 2002, “A General View of Construction Finite Volume Methodologies for Fluid Flow Simulations”, III Escola de Primavera em Transição e Turbulência, 23-27 Setembro, 2002.